Electronic Supplementary Information

Towards a high MnO_2 loading and gravimetric capacity from proton-coupled Mn^{4+}/Mn^{2+} reactions using 3D free-conducting conducting scaffold

Arvinder Singh,[a] Ozlem Sel,[b] Hubert Perrot,[b] Véronique Balland,[c] Benoît Limoges,[c] and Christel Laberty-Robert*[a]

[a] Chimie de la Matière Condensé**,** Sorbonne Université - CNRS, UMR 7574, 4 place Jussieu, 75005 Paris, France

[b] Laboratoire Interfaces et Systèmes Electrochimiques (LISE), Sorbonne Université - CNRS, UMR8235, 4 place Jussieu, 75005 Paris, France.

[c] Université de Paris, Laboratoire d'Electrochimie Moléculaire, UMR CNRS 7591, F-75013 Paris, France.

I. Experimental

i. Chemicals

N, N–dimethylformamide (DMF), and glacial acetic acid were purchased from CARLO ERBA Reagents. Polyacrylonitrile (PAN, Average M_W 150000), potassium acetate (BioUltra, ≥ 99.0%), potassium chloride (BioXtra ≥ 99.0%), and manganese (II) chloride (≥ 99%) were purchased from Sigma Aldrich.

ii. Preparation of carbon nanofibers (CNFs)

CNFs were prepared using the electrospinning technique as reported elsewhere.[S1-3] In brief, 10 wt% of PAN was first dissolved in DMF solvent at 75–80 °C until the solution became transparent and then stirred at room temperature overnight. A fixed volume (2.55 mL) of the as-prepared solution was electrospun at room temperature using a syringe at a fixed distance of ~15 cm between the needle tip and the grounded collector (aluminum foil). The applied voltage was ~18 kV, and the relative humidity was below 20% during the electrospinning process. The resultant polymeric nanofibers were peeled off from the collector and first stabilized in air at 280 °C for 5 h and finally carbonized at 1200 °C (heating rate of 5 °C/min) for 1 h in a horizontal tube furnace under steady Ar flow.

iii. Physical characterizations

Microstructural/morphological features were investigated using field emission gun scanning electron microscopy (SEM&FEG) (Zeiss, Supra 55) equipped with an energy dispersive spectrometer. For the estimation of the mean diameter of bare or MnO_2 covered CNFs from FEG-SEM images, a total of ca. 50 data points (diameter size) were collected using ImageJ software on 15-20 different NFs with 2-3 measurements on each fiber. XRD measurement was performed under ambient conditions using an X-ray diffractometer (Phillips PANanalytical X'Pert Pro) with Cu K_α radiation (λ = 1.54184 Å) source. Core-level X-ray photoelectron spectroscopy (XPS) spectra were collected using VG ESCALAB 250i-XL spectrometer equipped with a monochromatic Al K_α excitation source. XPS spectra were charge-corrected to the binding energy of the C 1s peak position (284.6 eV). Moreover, the fitting of the core-level spectra was done using CASAXPS software and with Shirley background.

iv. Electrochemical measurements

For the electrochemical characterization of as-prepared CNFs, we performed cyclic voltammetry (CV) and galvanostatic charge–discharge (GCD) analyses of 1 x 1 cm^2 electrode in 1 M KCl aqueous electrolyte using Ag/AgCl (sat. KCl) as the reference electrode, and Pt-mesh as the counter electrode. This measurement is done with a self-standing CNF electrode in a conventional 3-electrode cell. The cell was controlled by biologic potentiostat interfaced with EC lab software. The areal capacitance of CNFs was estimated using the following relations:[S4]

$$C\ (F/cm^2) = i_a /(v \cdot A) \quad \text{(for CV)} \qquad \text{(S1)}$$

$$C\ (F/cm^2) = I \cdot \Delta t/\Delta E \quad \text{(for GCD)} \qquad \text{(S2)}$$

where i_a is the observed average current at middle potential (0.3 V in the present case), v is the scan rate (V/s), A is the geometric electrode area (cm^2), I is the applied current density (A/cm^2), Δt is the discharge or charge time, and ΔE is the voltage window. All current densities refer to the geometric surface area.

To monitor the deposition–dissolution of MnO_2 on the bare gold and CNFs covered gold electrode, the gold-patterned quartz (Au-quartz) substrates of 9 MHz (gold electrode geometric surface area of 0.2 cm^2; AWS, Valencia, Spain) were used as working electrodes with or without CNFs coverage. For CNFs coverage on the gold electrode, CNFs were ground and dispersed in ethanol using an ultrasonication bath for 20–30 min to get homogeneous dispersion. CNFs were then deposited on the gold electrode using the "drop-casting" method at room temperature. We estimated the mass of the deposited CNFs by measuring a change in the frequency (Δf) of the resonator (in air) due to CNFs deposition and then by converting Δf to Δm using the Sauerbrey equation. The Sauerbrey equation is given below:

$$\Delta f = -k_s.\Delta m \qquad \text{(S3)}$$

where k_s is the experimental calibration constant 16.6 x 10^7 $Hz/(g.cm^{-2})$ as estimated previously.[S5-7] The estimated mass of the deposited CNFs was ~35 $\mu g/cm^2$. The galvanostatic experiments were performed in a custom-made EQCM cell using Pt–grid as counter electrode and Ag/AgCl (sat. KCl) as the reference electrode. The EQCM cell was controlled by an AUTOLAB GP-11 potentiostat interfaced with the GPES software. For all the measurements in 3-electrode EQCM cell, we used aqueous 1 M acetate (CH_3COOH/CH_3COOK ; pK_a = 4.79) buffer (pH = 5)

solution with 10 mM concentration of Mn^{2+} ($MnCl_2$•4 H_2O) as electrolyte. For the CNF covered gold electrode, an area factor is introduced in comparison to bare gold, as coverage of CNFs on the 2D gold electrode significantly increases the active surface area. For PAN-derived non-activated CNFs with an average diameter of < 200 nm, the typical specific surface area is ~35 m^2/g as reported previously.[S8-10] For a CNF loading of ~35 µg/cm^2 on the gold, we thus expect a surface area enhancement of ~12 (35 (µg/cm^2) × 35 (m^2/g) = 12.25). Therefore, upscaling the electrodeposition method from 2D gold to 3D CNF was achieved using an area factor of 12 for the CNF covered gold electrode. Accordingly, the galvanostatic experiments were performed at 50 µA/cm^2 current density at the 2D gold electrode, with a charge fixed in the range 3–15 mC/cm^2. At the 3D CNF electrode, the current density was 0.6 mA/cm^2 (equivalent to 50 µA per theoretical enhanced surface area) and the charge was fixed to 36–180 mC/cm^2.

For the galvanostatic cycling of free-standing 3D CNFs, we used a standard 3-electrode cell with CNFs as working electrode (area 1 cm^2, thickness ~150 µm, ~1.54 mg_{CNF}/cm^2), Ag/AgCl (sat. KCl) as the reference electrode, Pt mesh as the counter electrode, and 7 mL volume of 0.1 (or 0.15) M Mn^{2+} pre-equilibrated in a 1 M acetate buffer as electrolyte (pH 5). For the galvanostatic cycling in two-electrode cell configurations, we used same set-up with Zn foil (Goodfellow Cambridge Limited) as counter electrode (1 cm x 1.5 cm), CNFs as working electrode (area 1 cm^2, thickness ~180 µm, ~1.76 mg_{CNF}/cm^2), and 7 mL volume of 0.15 M Mn^{2+} + 0.25 M Zn^{2+} (chloride) + 1 M acetate buffer as electrolyte (pH = 4.85). The GCD cycling for Zn/MnO_2-CNFs configuration was performed at ± 1 mA/cm^2 for Q_{charge} = 5 C/cm^2 and with a fixed lower cut-off potential of 0.6 V *vs*. Zn/Zn^{2+}. Before use, the Zn foil was cleaned with 2 M HCl (for 5 min) and subsequently with acetone and ethanol.

II. Characterization of electrospun CNFs

In this work, we have used electrospun CNFs on the gold electrode of quartz crystal resonator as a 3D substrate for the electrodeposition-electrodissolution of MnO_2 in mild aqueous electrolyte. The morphological characterization of the as-prepared CNFs was done by SEM-FEG, which is shown in Fig. S1(a).

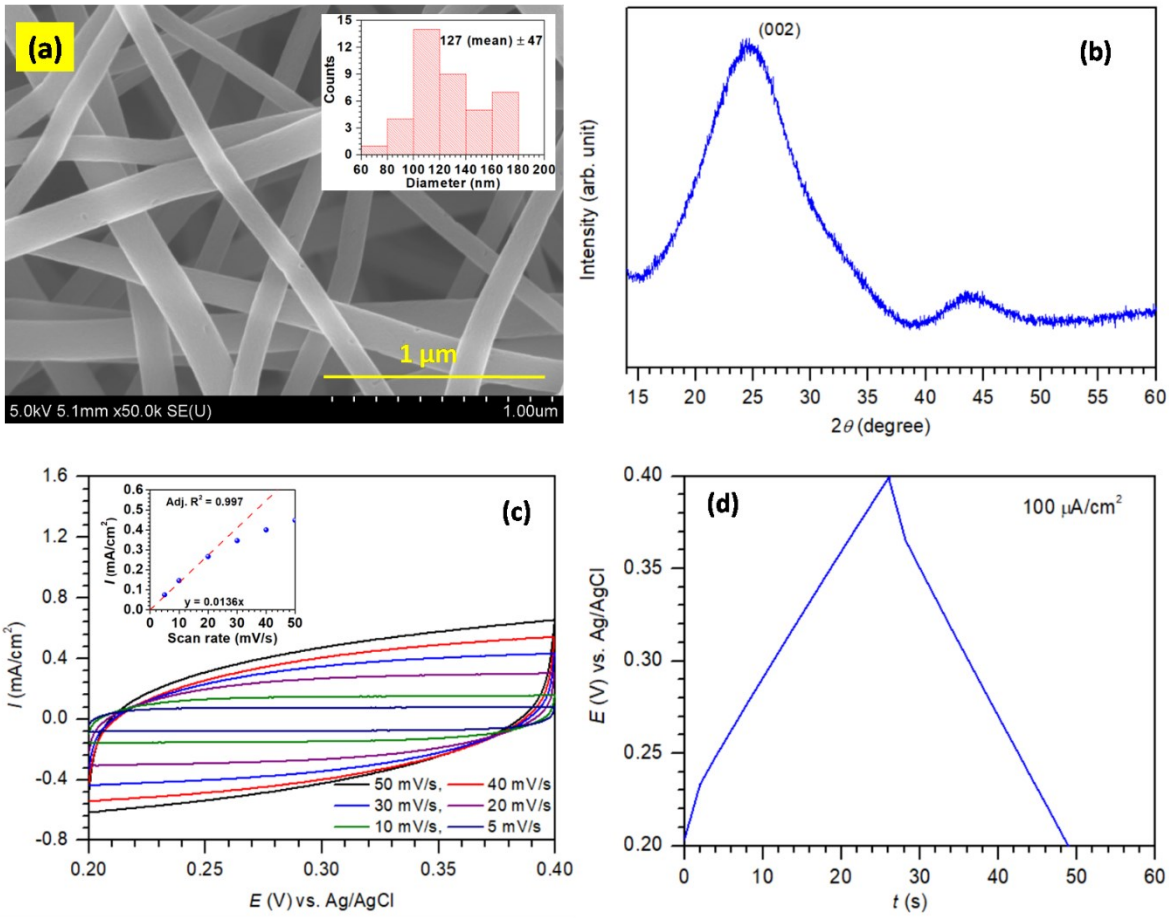
(a)
127 (mean) ± 47
Counts
Diameter (nm)
1 µm
5.0kV 5.1mm x50.0k SE(U)
1.00um
(b)
(002)
Intensity (arb. unit)
2θ (degree)
(c)
Adj. R² = 0.997
y = 0.0136x
Scan rate (mV/s)
I (mA/cm²)
50 mV/s, 40 mV/s
30 mV/s, 20 mV/s
10 mV/s, 5 mV/s
E (V) vs. Ag/AgCl
(d)
100 µA/cm²
E (V) vs. Ag/AgCl
t (s)

Fig. S1 Characterization of electrospun carbon nanofibers (CNFs) carbonized at 1200 °C. (a) FEG-SEM image of CNFs and distribution of fiber diameter (inset) estimated using Image J software, (b) XRD pattern of CNFs carbonized at 1200 °C, (c) Cyclic voltammetric (CV) curves recorded from 0.2 to 0.4 V at different scan rates (*i.e.*, 5, 10, 20, 30, 40 and 50 mV/s) in a 1 M KCl aqueous electrolyte with an electrode loaded with 3.96 mg_{CNF}/cm^2. The inset to (c) shows the variation of the current density (measured at +0.3 V) as a function of scan rate, and (d) galvanostatic charge-discharge (GCD) curve recorded from 0.2 to 0.4 V at ± 100 $\mu A/cm^2$ in a 1 M KCl aqueous electrolyte for the same electrode. For CV and GCD, an Ag/AgCl (sat. KCl) and a Pt-mesh were used as the reference and counter electrodes, respectively.

The FEG-SEM image collected for CNFs shows that NFs have a smooth surface. The distribution of diameter for CNFs is shown in the inset of Fig. S1(a). CNFs exhibit a mean diameter of 127 ± 47 nm. The typical BET surface area for PAN-based electrospun CNFs with an average diameter below 200 nm is ~35 m^2/g, as reported previously.[S10] The XRD pattern of CNFs (Fig. S1(b)) shows a broad peak centered at $2\theta = 24.5°$, which represents the (002) plane.[S11] The calculated d_{002}-spacing from the Bragg's law ($2 \cdot d \cdot \sin\theta = n \cdot \lambda$, $\lambda = 0.15418$ nm) is around 0.3634 nm, which is higher but not so far from the d_{002} value for ideal graphitic carbon (0.344 nm).[S11] Thus, up to some extent, CNFs carbonized at 1200 °C is similar to turbostratic carbon and exhibits short-range ordered (graphitic) domains, similar to what is reported previously for CNFs carbonized at ≥ 1000 °C.[S8, 11]

For the electrochemical characterization of free-standing CNFs, electrodes were first scanned between 0.2 to 0.4 V at different scan rates in a 1 M KCl electrolyte (pH = 6.4). The observed CV responses are shown in Fig. S1(c). The well-defined rectangular CV curves without any faradaic peaks indicate the reversible formation of the double-layer capacitor at the CNFs/electrolyte interface. The observed current density at the slowest scan rates varies linearly, which is characteristic of the charge/discharge of the pure double-layer capacitance of a high surface area electrode without significant interference of the ohmic drop.[S12] The areal capacitance of CNFs estimated from the CVs recorded at the slowest scan rates (*i.e.*, from the slope of the linear fit in the inset of Fig S1(c)) is ca. 13.6 mF/cm^2 (equivalent to 3.4 F/g), which agrees with the reported values for carbon materials with specific surface area $S_{BET} < 50$ m^2/g.[S13]

Fig. S1(d) shows galvanostatic (100 μA/cm^2) charge-discharge curves for CNFs electrode in 1 M KCl electrolyte. The observed nearly symmetrical V-shaped GCD response further corroborates the charge/discharge of a pure double-layer capacitance. The areal capacitance of CNFs estimated from GCD is 11.4 mF/cm^2 (2.9 F/g), corroborating thus well the CV results. The coverage of the gold electrode with electrospun CNFs brings a substantial improvement in the active sites for nucleation/growth, thus affecting the MnO_2 deposition-dissolution process.

III. XRD pattern of the electrodeposited MnO_2

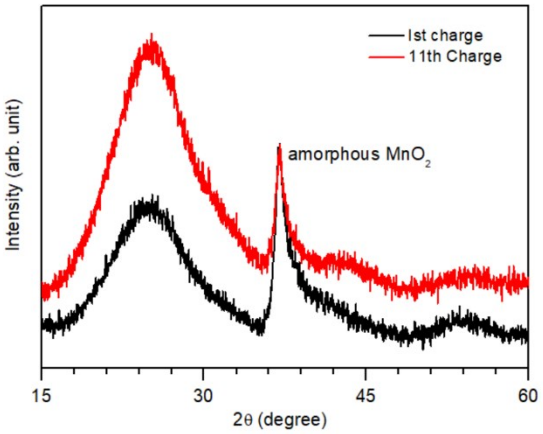

Fig. S2 The XRD pattern of the fully charged free-standing CNF electrodes after 1st and 11th electrodeposition process for Q_{charge} of 180 mC/cm^2. The (111) peak of the gold (Au-quartz substrate) appears at 2θ = 38.1°,[S14] which overlaps with the broad peak of the electrodeposited amorphous MnO_2 centered at 2θ = 37°. Therefore, we used free-standing CNFs to perform phase analysis of the electrodeposited MnO_2. The broad peak centered at 2θ = 24.5° is assigned to the (002) plane of CNFs.

IV. Cross-section FEG-SEM image of CNF covered Au-quartz electrode after discharge

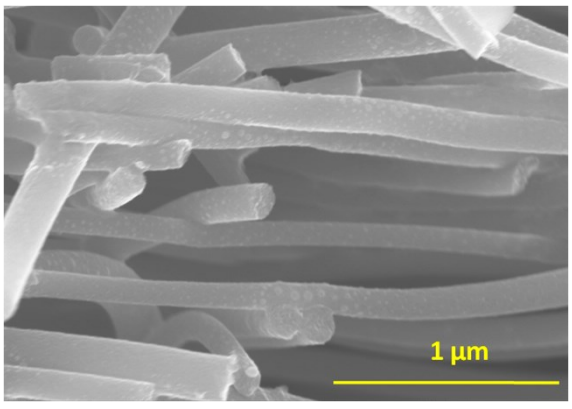

Fig. S3 Cross-section FEG-SEM image of CNF-covered Au-quartz electrode after electrodissolution of MnO_2 for Q_{charge} of 180 mC/cm^2 (discharged state).

V. Mn 3s XPS spectra of free-standing CNFs after electrodeposition of MnO_2

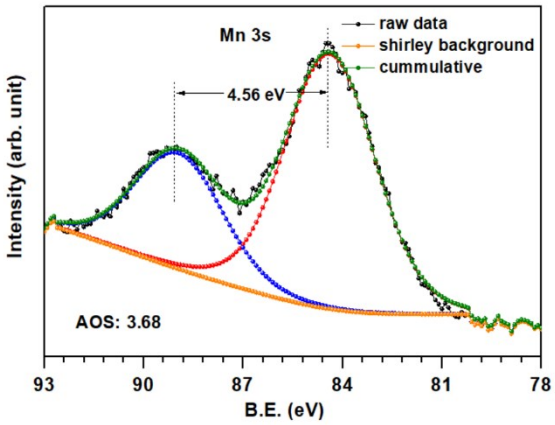

Fig. S4 Core-level Mn 3s XPS spectra of free-standing CNFs after electrodeposition of MnO_2 for Q_{charge} of 180 mC/cm^2 (charged state). The binding energy (B.E.) of Au 4f doublet exactly overlaps with that of Mn 3s doublet. Therefore, we performed XPS on the MnO_2 covered free-standing CNF electrodes after the first charge.

VI. GCD for different loads and corresponding Δf *vs.* Q_{charge} (loads) profile for CNF covered Au-quartz electrodes

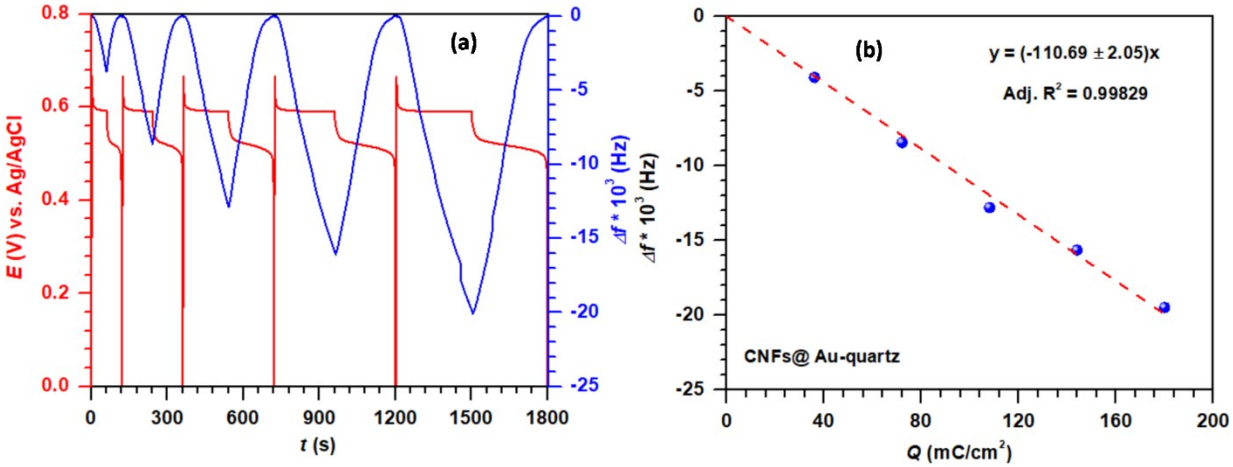

Fig. S5 (a) Galvanostatic (0.6 mA/cm^2) charge-discharge curves with different loads (Q_{charge}) of 36, 72, 108, 144, and 180 mC/cm^2 applied successively on the same electrode and the simultaneous QCM monitoring for the CNF-covered Au-quartz electrode. (b) Corresponding Δf *vs.* Q_{charge} response. The linearity of this response indicates the validity of the gravimetric regime of QCM and thus the use of the Sauerbrey equation (eq S3) for mass estimation.

VII. GCD cycling and simultaneous QM monitoring on the bare Au-quartz electrode

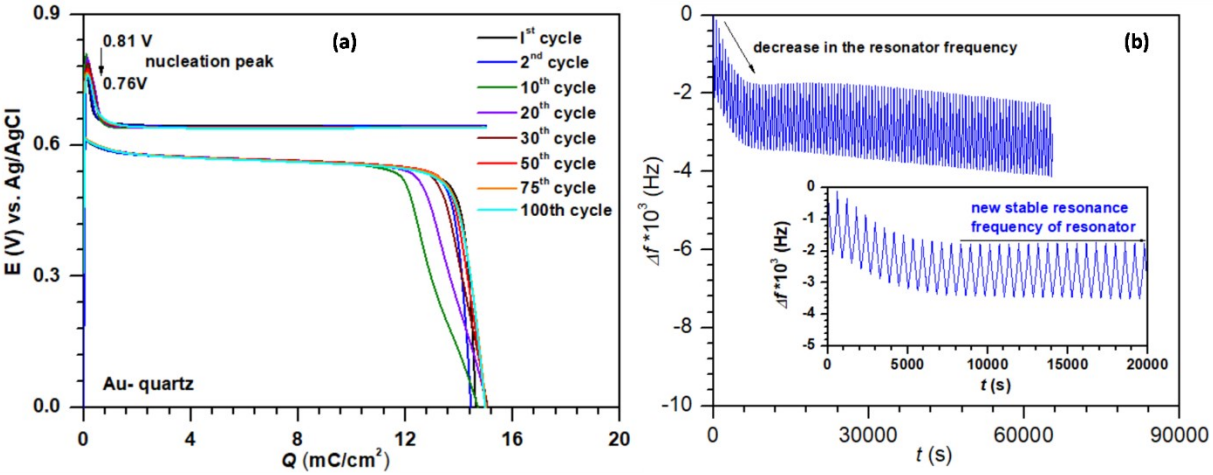

Fig. S6 (a) GCD cycles (shown for eight specific cycles) and (b) simultaneous QCM monitoring (frequency change) for electrodeposition-electrodissolution of MnO_2 on the bare Au-quartz electrode at 50 µA/cm^2 for a total load (Q_{charge}) of 15 mC/cm^2. The inset in (b) shows the frequency change for the initial few cycles.

VIII. GCD for different loads and corresponding Δ*f vs.* Q_{charge} (loads) profile for bare Au-quartz electrodes

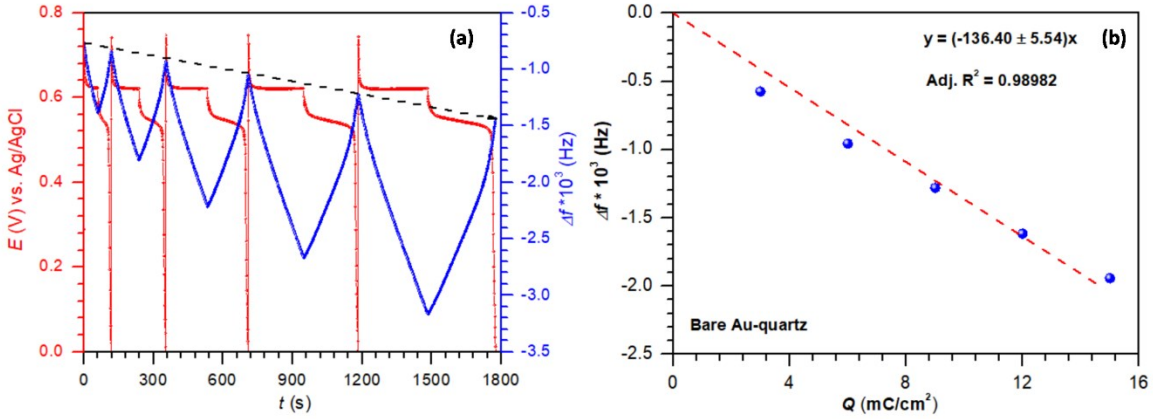

Fig. S7 (a) Galvanostatic (50 µA /cm^2) charge-discharge curves with different loads (Q_{charge}) of 3, 6, 9, 12, and 15 mC/cm^2 applied successively on the same electrode and the simultaneous QCM trace for the bare Au-quartz electrode. (b) Corresponding Δ*f vs.* Q_{charge} response.

Fig. S5 (b) shows the change in the frequency (Δ*f*) of the resonator during the electrodeposition-electrodissolution of MnO_2 on the 2D bare Au-quartz electrode while cycling galvanostatically at 50 µA/cm^2 for a total Q_{charge} of 15 mC/cm^2 (Fig. S5 (a)). On the bare gold electrodes, the frequency profile of the resonator is progressively shifted for the first 20-25 cycles and then stabilized to a

new resonance frequency. The Δ*f* of the resonator does not come back to its initial value for the first 20-25 cycles as evidenced by the low C.E. values of ≤ 90%. It is noteworthy that the bare Au-quartz is under the gravimetric regime during measurements as evidenced from the linear Δ*f vs.* Q_{charge} profiles (Fig. S6(b)) collected with different successive loads (Q_{charge}) of 3, 6, 9, 12, and 15 mC/cm^2 on the same electrode (Fig. S6(a)).[S15] Therefore, the initial shift of the resonance frequency (in liquid) during the first few cycles on the bare Au-quartz electrode can be attributed to the formation of a poorly electroactive layer of MnO_2, which does not electrodissolve during the discharge process. However, after 20 cycles, C.E. rises to ~99.5% and remains quite stable with negligible fading (0.5%) over 100 cycles, suggesting deposition/dissolution of a nearly constant quantity of MnO_2 over the poorly electroactive layer of MnO_2 (accumulated in the first 20 cycles). The nucleation potential on the bare 2D Au-quartz electrode is found to decrease gradually upon cycling (Fig. S5(a)), which further indicates an improvement in sites for nucleation and surface area of the bare Au-quartz electrode during cycling (thus formation and accumulation of poorly active MnO_2).

IX. FEG-SEM analysis of CNFs after electrodeposition of MnO_2 at different loads on the 3D free-standing CNF electrodes

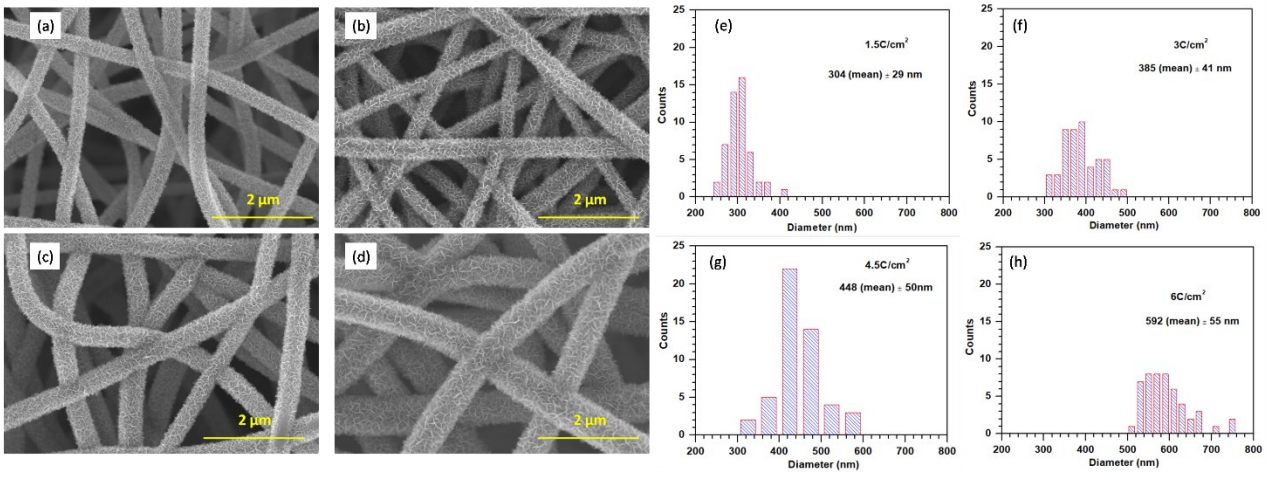

Fig. S8 (a-d) FEG-SEM images of free-standing CNFs after electrodeposition of MnO_2 at 1 mA/cm^2 for Q_{charge} of 1.5, 3, 4.5, and 6 C/cm^2, respectively. (e-h) Distribution and mean diameter size of CNFs after electrodeposition of MnO_2 at 1 mA/cm^2 for Q_{charge} of 1.5, 3, 4.5, and 6 C/cm^2, respectively.

X. Galvanostatic cycling on the 3D free-standing CNF electrodes at Q_{charge} of 3 C/cm^2

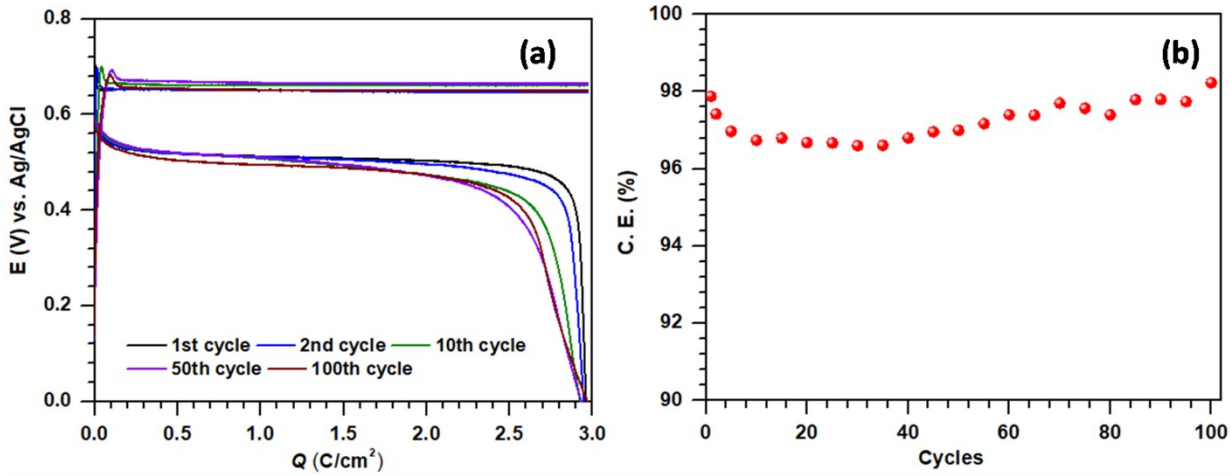

Fig. S9 (a) GCD cycles (shown for 5 specific cycles over 100) and (b) corresponding C.E. obtained during cycling on free-standing CNFs at Q_{charge} of 3 C/cm^2 in 1 M acetate buffer containing 0.1 M $MnCl_2$ (pH = 5).

XI. Galvanostatic cycling of Zn-MnO_2/CNF cell at Q_{charge} of 5 C/cm^2

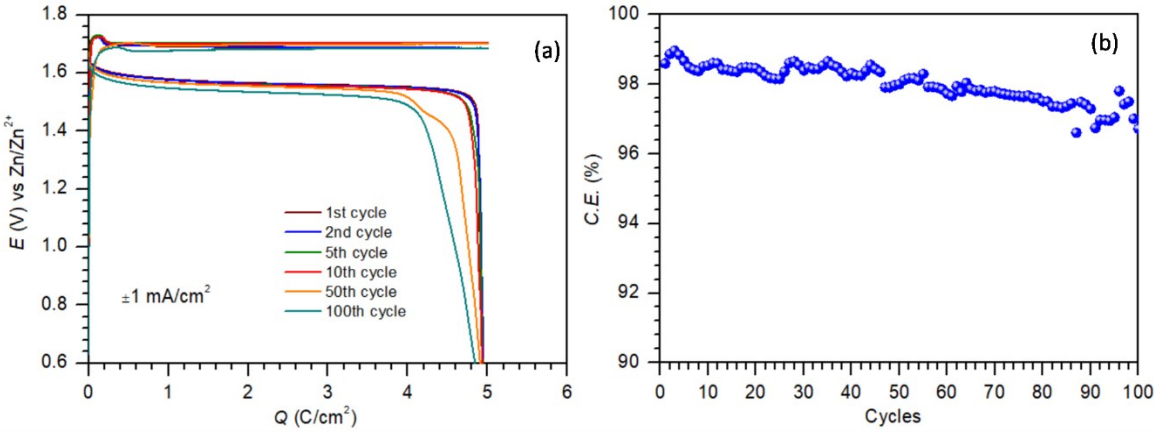

Fig. S10 (a) GCD cycles (shown for 6 specific cycles over 100) and (b) corresponding C.E. obtained in a two electrodes cell configuration. The Zn foil is used as counter electrode and free-standing CNFs (area 1 cm^2, thickness 180 µm, ~1.76 mg_{CNF}/cm^2) are used as working electrode. GCDs are collected at ± 1 mA/cm^2 for Q_{charge} of 5 C/cm^2 in 0.15 M $MnCl_2$ + 0.25 M $ZnCl_2$ + 1 M acetate buffer solution (pH = 4.85).

References:

S1 A. Singh and V. Kalra, *ACS Appl. Mater. Interfaces*, 2018, **10**, 37937-37947.

S2 A. Singh and V. Kalra, *J. Mater. Chem. A*, 2019, **7**, 11613-11650.
S3 A. Singh, A. Rafie and V. Kalra, *Sustainable Energy Fuels*, 2019, **3**, 2788-2797.
S4 A. Singh and A. Chandra, *Sci. Rep.*, 2016, **6**, 25793-25806.
S5 C. R. Arias, C. Debiemme-Chouvy, C. Gabrielli, C. Laberty-Robert, A. Pailleret, H. Perrot and O. Sel, *J. Phys. Chem. C*, 2014, **118**, 26551-26559.
S6 D. Aurbach and A. Zaban, *J. Electroanal. Chem.*, 1995, **393**, 43-53.
S7 K. Bizet, C. Gabrielli and H. Perrot, *Appl. Biochem. Biotechnol.*, 2000, **89**, 139-149.
S8 A. Gupta, S. R. Dhakate, P. Pal, A. Dey, P. K. Iyer and D. K. Singh, *Diamond Relat. Mater.*, 2017, **78**, 31-38.
S9 J. Sun, G. Wu and Q. Wang, *J. Appl. Polym. Sci.*, 2005, **97**, 2155-2160.
S10 D. Hussain, F. Loyal, A. Greiner and J. H. Wendorff, *Polymer*, 2010, **51**, 3989-3997.
S11 R. Schierholz, D. Kröger, H. Weinrich, M. Gehring, H. Tempel, H. Kungl, J. Mayer and R.-A. Eichel, *RSC Adv.*, 2019, **9**, 6267-6277.
S12 C. Costentin and J. M. Saveant, *Chem. Sci.*, 2019, **10**, 5656-5666.
S13 O. Barbieri, M. Hahn, A. Herzog and R. Kötz, *Carbon*, 2005, **43**, 1303-1310.
S14 S. Krishnamurthy, A. Esterle, N. C. Sharma and S. V. Sahi, *Nanoscale Res. Lett.*, 2014, **9**, 627-635.
S15 N. Shpigel, M. D. Levi and D. Aurbach, *Energy Storage Mater.*, 2019, **21**, 399-413.